

DETERMINATION OF DNA MELTING CURVES AND DIFFERENTIAL  
MELTING CURVES FROM CALORIMETRIC DATA

I. E. GRIGORYAN\*

*Chair of Molecular Physics YSU, Armenia*

For different types of DNA sequences it is demonstrated that a calorimetric melting curve calculated as a temperature dependence of a relative heat absorbance caused by DNA helix-coil transition is very close to the “real” melting curve that is the temperature dependence of the fraction of melted base pairs. There is the same closeness for the calorimetric differential melting curves (DMC) and the values of melting temperatures and temperature melting ranges. A simple procedure of recalculation of a calorimetric DMC into a real DMC is proposed.

**Keywords:** differential scanning calorimetry, high-resolution melting profiles, DNA plasmids, Calf Thymus DNA.

**Introduction.** As a tool for the measurement of DNA melting curves, differential scanning calorimetry (DSC) is more sensitive than UV absorption spectrophotometry. The advantage of DSC is a direct determination of differential melting curves (DMC) obtained from thermograms by subtraction of buffer baseline, sample baseline and normalization. However, there is a widely spread opinion that calorimetry has shortcomings that hinder exact determination of the melting curve, DMC, melting temperature and temperature melting range. The most important of them is the difference between the helix coil-transition enthalpies of *AT* and *GC* base pairs. Because of lower enthalpy of *AT* base pairs, the low temperature part of calorimetric DMC corresponding to *AT*-rich regions is lower than real DMC that is the first temperature derivative of the fraction of melted base pairs. The high temperature part corresponding to *GC*-rich regions is located above the real DMC. At the same time, there is no exact evaluation of the distortion value caused by this effect.

As the differential scanning calorimetry, UV registration of DNA absorption also does not measure the fraction of melted base pairs directly, various methods are required to escape experimental errors. However, the contribution to the total change of absorbance is approximately the same for *AT* and *GC* base pairs at  $\lambda=270\text{ nm}$  [1–3].

It is demonstrated in this study that the method of differential scanning calorimetry causes minor error in the determination of the melting curve, DMC, melting temperature and temperature melting range. A simple procedure of recalculation of a calorimetric DMC into a real DMC is proposed.

---

\* E-mail: inessgrigoryan@yahoo.com

**Materials and Methods.** Ultra pure Calf Thymus DNA prepared in the Laboratory of Prof. D.Y. Lando was used (protein<0.1%, RNA<0.1%, molecular mass ~30 MDalton). The properties of this DNA have been previously described [4]. High-resolution melting profiles were obtained using a model of differential scanning microcalorimeter DASM 4 (“Biopribor”, Russia) with a cell volume 0.5 ml. In the DSC experiments we followed standard procedures [5]. The melting was carried in 0.1 M NaCl, 5 mM Na<sub>2</sub>CO<sub>3</sub>, 0.05 mM EDTA, pH 7.

The fraction of melted base pairs  $\mathcal{G}(T)$  (melting curve) and its first derivative  $\mathcal{G}'_T(T)$  DMC called further in the text as "real" curves or dependences were obtained by theoretical calculations using the Poland–Fixman–Freire (PFF) approach [5, 6]. The calorimetric DMC  $\mathcal{G}'_{c_T}(T)$  was obtained from thermograms by subtraction of buffer baseline, sample baseline and normalization. The calorimetric melting curve  $\mathcal{G}_c(T)$  is calculated by integration of the calorimetric DMC, i.e. it is the temperature dependence of heat absorption normalized to total heat absorption caused by the DNA helix-coil transition. Both dependences can be expressed through the additional heat capacity caused by the helix-coil transition ( $\Delta C_p(T)$ ):

$$\mathcal{G}'_{c_T}(T) = \Delta C_p(T) / \int_{T_s}^{T_e} \Delta C_p(t) dt, \quad (1)$$

$$\mathcal{G}_c(T) = \int_{T_s}^T \mathcal{G}'_{c_T}(t) dt = \int_{T_s}^T \Delta C_p(t) dt / \int_{T_s}^{T_e} \Delta C_p(t) dt, \quad (2)$$

where  $T_s$  and  $T_e$  are the start and end of the temperature interval of the DNA helix-coil transition.

The PFF approach [5–7] was used for calculation of real melting curves for the two sets of parameters. The first set corresponds to equal entropies of the helix-coil transition for AT and GC base pairs:  $T_{AT}=65.2^\circ\text{C}$ ,  $T_{GC}=107.8^\circ\text{C}$ ,  $H_{AT}=8.4 \text{ kcal}/(\text{mol}\cdot\text{bp})$ ,  $H_{GC}=9.5 \text{ kcal}/(\text{mol}\cdot\text{bp})$ ,  $S_{AT}=S_{GC}=24.8 \text{ cal}/(\text{mol}\cdot\text{bp}\cdot\text{K}^{-1})$  [8]. The second set was used for EcoRI-cut pBR322 DNA for the illustration example, in which high difference in enthalpies is taken ( $H_{GC}-H_{AT}=4 \text{ kcal}/(\text{mol}\cdot\text{bp})$ ):  $H_{AT}=9 \text{ kcal}/(\text{mol}\cdot\text{bp})$ ,  $H_{GC}=13 \text{ kcal}/(\text{mol}\cdot\text{bp})$ ,  $S_{AT}=26.60 \text{ cal}/(\text{mol}\cdot\text{bp}\cdot\text{K}^{-1})$ ,  $S_{GC}=34.12 \text{ cal}/(\text{mol}\cdot\text{bp}\cdot\text{K}^{-1})$ ,  $T_{AT}=65.2^\circ\text{C}$ ,  $T_{GC}=107.8^\circ\text{C}$ .

### Results and Discussion.

*An exact representation of  $\mathcal{G}_c$ .* A model of  $N$  base pairs with two types of stability (AT and GC) is used. Such simple types of heterogeneity are the most suitable for the assessments carried out in this study. For this model, the temperature dependence of the heat absorption caused by DNA helix-coil transition can be represented in the following way:

$$H(T) = N_{AT_1}(T)H_{AT} + N_{GC_1}(T)H_{GC}, \quad (3a)$$

$$N_1 = N_{AT_1} + N_{GC_1}, \quad (3b)$$

where  $N_1$ ,  $N_{AT_1}$ ,  $N_{GC_1}$  are the numbers of melted base pairs: total, AT and GC respectively,  $H_{AT}$  and  $H_{GC}$  are the enthalpy of the helix-coil transition for AT and GC base pair.

It is obvious that  $H(T)$  is close to zero at  $T < T_s$  and to  $H_f$  at  $T > T_e$ , where  $H_f$  is the enthalpy of the helix-coil transition:

$$H_f = N_{AT}H_{AT} + N_{GC}H_{GC}, \quad (4)$$

$N_{AT}$  and  $N_{GC}$  are the total numbers of  $AT$  and  $GC$  base pairs respectively.

The real melting curve  $\mathcal{G}(T)$  and the melting curve calculated from calorimetric data  $\mathcal{G}_c(T)$  are the following:

$$\mathcal{G}(T) = N_l / N, \quad (5a)$$

$$\mathcal{G}_c(T) = H(T) / H_f. \quad (5b)$$

*An Approximate Representation of  $\mathcal{G}_c$ .* Let the temperature  $T_l$  corresponds to the melting out of the DNA regions with the average  $GC$  composition  $x_l$ . At that temperature the majority of regions with  $x < x_l$  are almost fully melted. If  $x > x_l$ , the regions are almost fully helical. It is obvious that

$$x_l = (T_l - T_{AT}) / (T_{GC} - T_{AT}). \quad (6)$$

The average per base pair enthalpy for those regions ( $H_l(T_l)$ ):

$$H_l(T_l) = (1 - x_l)H_{AT} + x_lH_{GC} = H_{AT} + x_l(H_{GC} - H_{AT}). \quad (7)$$

$H_l(T_l)$  can be also represented in the following way:

$$H_l(T_l) = H_{AT} + \frac{T_l - T_{AT}}{T_{GC} - T_{AT}}(H_{GC} - H_{AT}). \quad (8)$$

Using  $H_l(T_l)$  one can obtain the heat absorption at a given temperature ( $H(T)$ ) and the total absorption caused by the DNA helix-coil transition ( $H_f$ ), and then calculate  $\mathcal{G}_c(T)$  using Eq. (5b):

$$H(T) = N \int_{T_s}^T H_l(T_l) \mathcal{G}'_{T_l}(T_l) dT_l, \quad (9)$$

$$H_f = N \int_{T_s}^{T_e} H_l(T_l) \mathcal{G}'_{T_l}(T_l) dT_l. \quad (10)$$

Let consider the case of equal entropies of the helix-coil transition for  $AT$  and  $GC$  base pairs ( $S_{AT}=S_{GC}=S$ ) that was used in some thermodynamic studies [8] and obtain the following simplified expressions for  $H_l(T_l)$ ,  $H(T)$  and  $H_f$ :

$$H_l(T_l) = T_l S, \quad (11)$$

$$H(T) = NS \cdot \int_{T_s}^T T_l \mathcal{G}'_{T_l}(T_l) dT_l, \quad (12)$$

$$H_f = NS \cdot \int_{T_s}^{T_e} T_l \mathcal{G}'_{T_l}(T_l) dT_l = NS\bar{T}, \quad (13)$$

where

$$\bar{T} = \int_{T_s}^{T_e} T \mathcal{G}'_T(T) dT, \quad (14)$$

The integral (14) is widely used in different thermodynamic studies [9], and parameter  $\bar{T}$  is representing the average melting temperature, which can be strongly different from melting temperature. Then  $\mathcal{G}_c(T)$  can be expressed using Eqs. (11)–(14):

$$\mathcal{G}_c(T) = H(T)/H_f = \frac{\int_{T_s}^T T_l \mathcal{G}'_{c_r}(T_l) dT_l}{\bar{T}}. \quad (15)$$

Differentiation of Eq. (15) gives an expression for DMC registered with differential scanning calorimetry Eq. (16):

$$\mathcal{G}'_{c_r}(T) = \mathcal{G}'_c(T/\bar{T}). \quad (16)$$

Using Eq. (16), one obtains calorimetric DMC from the real DMC. However, the reverse procedure of transformation of a calorimetric DMC into a real one is more necessary. For the transformation, it is necessary to express through experimental function  $\mathcal{G}_c(T)$ . To do this, let us transpose  $T$  into the left part of Eq. (16) and integrate the obtained expression:

$$\int_{T_s}^{T_g} T^{-1} \mathcal{G}'_{c_r}(T) dT = \bar{T}^{-1}. \quad (17)$$

As a result one obtains  $\bar{T}$  and  $\mathcal{G}'_T(T)$  from  $\mathcal{G}'_{c_r}(T)$ :

$$\bar{T} = \left[ \int_{T_s}^{T_g} T^{-1} \mathcal{G}'_{c_r}(T) dT \right]^{-1}, \quad (18)$$

$$\mathcal{G}'_T(T) = \mathcal{G}'_{c_r}(T)(\bar{T}/T). \quad (19)$$

The difference between real and calorimetric DMC

$$\mathcal{G}'_T(T) - \mathcal{G}'_{c_r}(T) = \mathcal{G}'_{c_r}(T)(\bar{T}/T) - \mathcal{G}'_{c_r}(T) = \mathcal{G}'_{c_r}(T)(\bar{T}/T - 1). \quad (20)$$

**Results of Calculation.** As follows from Eq. (16), calorimetric DMC is located lower, than real DMC at  $T < \bar{T}$  and higher at  $T > \bar{T}$ . It is also obvious that a stronger difference of a calorimetric melting curve from the corresponding real melting curve

occurs for a larger temperature melting range Eq. (20). It can be seen from Eq. (20), that the deviation is independent of the  $H_{AT}$  and  $H_{GC}$  values. However, there is an implicit dependence, because both  $\mathcal{G}'_T(T)$  and  $\mathcal{G}'_{c_r}(T)$  are dependent on the enthalpies.

Recalculation of experimental calorimetric curve  $\mathcal{G}'_c(T)$  into a real one  $\mathcal{G}'_T(T)$  using Eqs. (18), (19) was carried out for Calf Thymus DNA (Fig. 1, A). The melting temperature and temperature melting range were also calculated for both types of curves, real and calorimetric. As follows from the figure, the experimental calorimetric curves ( $\mathcal{G}_c, \mathcal{G}'_{c_r}$ )

and real curves ( $\mathcal{G}, \mathcal{G}'_T$ ) calculated from them are very close. The difference in melting temperature and melting range for two types of curves also does not exceed  $0.05^\circ\text{C}$ . It means that the recalculation is not necessary,

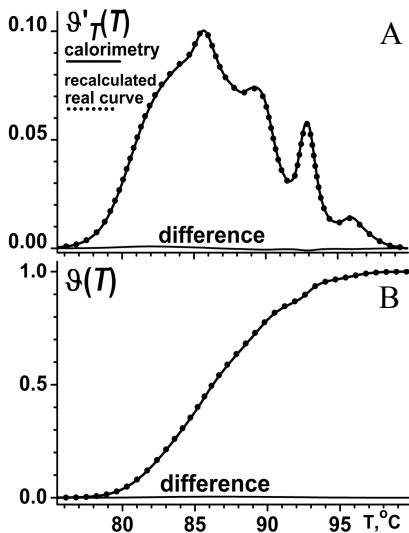


Fig. 1. Experimental normalized calorimetric melting curve from Calf Thymus, and results of its recalculation into real curve: A – differential melting curves; B – melting curves.

neither for the curves nor for their parameters.

As follows from Eq. (20), high deviation between real and calorimetric melting curves can be obtained for extremely high degree of DNA heterogeneity. As an example of that case, DNA of 10 *kbp* that includes two random blocks of 5 *kbp* was considered. The sequence of both blocks is random, and the *GC* content is different (0.25 and 0.75). Real curves were calculated using PFF approach and then recalculated into calorimetric curves using Eq. (16). Calculation gives the difference in real and calorimetric melting temperature of only 0.3°C. For the temperature melting range, the difference is equal to 0.8°C that is approximately 3% of the melting range (Fig. 2).

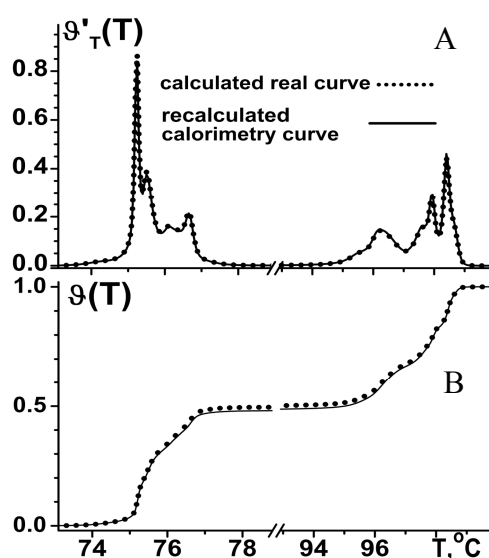


Fig. 2. Real melting curve and its first derivative calculated with the PFF approach for DNA of 10 *kbp* that includes two blocks each of 5 *kbp* with random sequence and *GC*=0.25 and 0.75. The calorimetric curves obtained from real ones using Eqs.(14), (16).  $T_{AT}=65.2^{\circ}\text{C}$ ,  $T_{GC}=107.8^{\circ}\text{C}$ ,  $H_{AT}=8408 \text{ cal}/(\text{mol}\cdot\text{bp})$ ,  $H_{GC}=9466 \text{ cal}/(\text{mol}\cdot\text{bp})$ ,  $S_{AT}=S_{GC}=24.8 \text{ cal}/(\text{mol}\cdot\text{bp}\cdot\text{K}^{-1})$ :

A – differential melting curves; B – melting curves.

Direct theoretical calculation of calorimetric ( $\mathcal{G}_c, \mathcal{G}'_c$ ) and real curves ( $\mathcal{G}, \mathcal{G}'_T$ ) with no requirements of  $S_{AT}$  and  $S_{GC}$  equality was also carried out for the sequence EcoRI-cut pBR322 and the case of very large difference in enthalpies:  $H_{AT}=9000 \text{ kcal}/(\text{mol}\cdot\text{bp})$ ,  $H_{GC}=13000 \text{ kcal}/(\text{mol}\cdot\text{bp})$ ,  $S_{AT}=26.60 \text{ cal}/(\text{mol}\cdot\text{bp})$ ,  $S_{GC}=34.12 \text{ cal}/(\text{mol}\cdot\text{bp})$ ,  $T_{AT}=65.2^{\circ}\text{C}$ ,  $T_{GC}=107.8^{\circ}\text{C}$ . Such large difference occurs between enthalpies of the most *GC* (*CG*) and less *TA* (*AT*) stable nearest neighbors of base pairs [2]. Even in this limiting case, the difference between two types of curves is very small (not shown).

Thus, the results of our work demonstrate that melting curve calculated as a relative heat absorbance caused by DNA helix-coil transition  $\mathcal{G}_c(T)$  is very close to the fraction of melted base pairs  $\mathcal{G}(T)$  and can be used without any recalculation. The same closeness for the calorimetric differential melting curves, and the values of melting temperatures and temperature melting ranges is demonstrated.

I am grateful to Prof. D.Y. Lando for supervisory leadership and for kind providing of ultrapure Calf Thymus DNA, to Prof. S.G. Haroutiunian and Prof. Y.B. Dalyan for their kind support.

*This work was supported by Belarusian-Armenian grants (X11Arm-013 and 11RB-017).*

*Received 19.01.2013*

#### REFERENCES

1. **Blake R.D., Hydorn T.G.** Spectral Analysis for Base Composition of DNA Undergoing Melting. // *J. Biochem. Biophys. Methods.*, 1985, v. 11, № 6, p. 307–316.
2. **Blake R.D., Delcourt S.G.** Electrostatic Forces at Helix-Coil Boundaries in DNA. // *Biopolymers*, 1990, v. 29, № 2, p. 393–405.
3. **Vardevanyan P.O., Karapetyan A.T., Terzikyan G.A., Vardapetyan R.R., Danielyan E.A.** Differential Melting Curves of DNA: Reliability of Extrema. // *Biopolymers and Cell*, 1990, v. 6, № 4, p. 48–51.
4. **Lando D.Y., Egorova V.P., Krot V.I., Akhrem A.A.** Determination of Protein Contaminants in DNA Preparations of High Purity. // *Molec. Biol.*, 1996, v. 30, № 3, p. 701–706.
5. **Poland D.** Recursion Relation Generation of Probability Profiles for Specific-Sequence Macromolecules with Long-Range Correlation. // *Biopolymers*, 1974, v. 13, № 9, p. 1859–1871.
6. **Fixman M., Freire J.J.** Theory of DNA Melting Curves. // *Biopolymers*, 1977, v. 16, № 12, p. 2693–2704.
7. **Volker J., Blake R.D., Delcourt S.G., Breslauer K.J.** High-Resolution Calorimetric and Optical Melting Profiles of DNA Plasmids: Resolving Contributions from Intrinsic Melting Domains and Specifically Designed Inserts. // *Biopolymers*, 1999, v. 50, № 3, p. 303–318.
8. **Wartell R.M., Benight A.S.** Thermal Denaturation of DNA Molecules: a Comparison of Theory with Experiment. // *Physics Reports*, 1985, v. 126, № 2, p. 67–107.
9. **Karapetian A.T., Vardevanian P.O., Frank-Kamenetskii M.D.** Enthalpy of Helix-Coil Transition of DNA: Dependence on Na<sup>+</sup> Concentration and GC-content. // *J. Biomol. Struct. Dyn.*, 1990, v. 8, № 1, p. 131–138.